Y-Band (170-260 GHz) Tunable CW IMPATT Diode Oscillators

CHENTE CHAO, MEMBER, IEEE, ROBERT L. BERNICK, MEMBER, IEEE, EDWARD M. NAKAJI, MEMBER, IEEE, ROBERT S. YING, MEMBER, IEEE, KENNETH P. WELLER, MEMBER, IEEE, AND DON H. LEE, MEMBER, IEEE

Abstract—**This paper describes circuit, packaging, and device techniques used in the development of tunable CW IMPATT diode oscillators in the 170–260 GHz range. A quartz standoff package with optimum values for parasitics has been developed. A tuning range of nearly 30 GHz has been achieved with an IMPATT diode in such a package.**

Introduction

RECENTLY, significant progress in output power and conversion efficiency has been achieved with IMPATT diode oscillators in both the CW and pulsed modes of operation at frequencies above 200 GHz. A CW output power of 50 mW at 202 GHz with a 1.3-percent conversion efficiency and a peak pulsed power of 520 mW at 214 GHz with a 2.6-percent conversion efficiency have been reported separately by different research groups [1], [2]. At these frequencies, because of the very short wavelength involved, chip-level circuit design is required. This paper describes the application of such a design approach to the development of CW IMPATT oscillators at *Y*-band (170–260 GHz) frequencies [3]. Circuit and package development, as well as diode design and characterization, and RF tuning characteristics of the oscillators are described.

Device Design and Fabrication

The diodes used in the present work have an ion-implanted double-drift-region (DDR) p^+-p-n-n^+ doping profile. The profile is formed by growing epitaxially a thin n layer on an arsenic doped ⟨111⟩ Si substrate wafer. The p-type region is fabricated by overcompensating with implanted boron ions [4]. The p^+ contact layer is formed by a shallow low-temperature diffusion of boron. These steps are processes normally used to fabricate millimeter wave IMPATT diodes. For *Y*-band frequencies, special attention must be given to substrate thinning and to minimizing unswept active regions.

At high frequencies, the RF loss of the device due to the n^+ substrate can be significant. This loss results from the series resistance of the substrate due to skin effects [5]. The substrate series resistance R_s is given by

$$R_s = \frac{\rho_s t}{\pi\delta(D-\delta)}$$

Manuscript received May 27, 1977. This work was supported in part by the Air Force Avionics Laboratories, Wright-Patterson AFB, Dayton, OH, under Contract F33615-76-C-1100, and in part by the U.S. Army Ballistic Research Laboratories, Aberdeen Proving Ground, MD, under Contract DAAD05-76-C-0744.

The authors are with Torrance Research Center, Hughes Aircraft Co., Torrance, CA 90509.

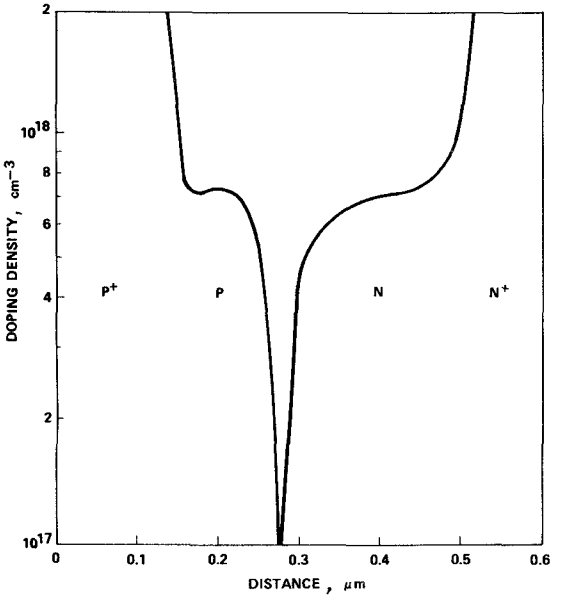

Fig. 1. Diode doping profile.

where ρ_s is the resistivity of the substrate, t the thickness, δ the skin depth, and D the diameter of the diode. At 225 GHz, for example, the skin depth is 3.4 μm. Taking D to be 25 μm and ρ_s to be 0.001 $\Omega \cdot$ cm, a thickness of even 10 μm will give a series resistance of 0.43 Ω. This is comparable to the diode negative resistance at 225 GHz and, therefore, must be minimized. For this reason, both chemical etch and syton polishing have been used to thin the substrates of diodes to approximately 5 μm.

Another important contribution to loss is due to the unswept active regions of diode. Because of the very high frequency of operation, the total active region of the IMPATT diode is only about 0.25 μm wide. The realization of the desired doping profile, and the elimination of the positive resistance associated with the unswept epitaxial region at the device-operating level are difficult, even with state-of-the-art technology. The accuracy required for determining the diode-doping profile approaches the resolution of the capacitance–voltage (C–V) method commonly used in profiling the diode. In order to achieve diodes which are just at punchthrough at the operating current level, the profile design for the devices was initially based on standard transit time considerations and was optimized empirically by varying the doping level of the active regions and by adjusting the diffusion time of the p^+ region. The doping profile C–V data has been gathered from those lots which have shown good RF performance. Fig. 1 shows a DDR doping profile of a

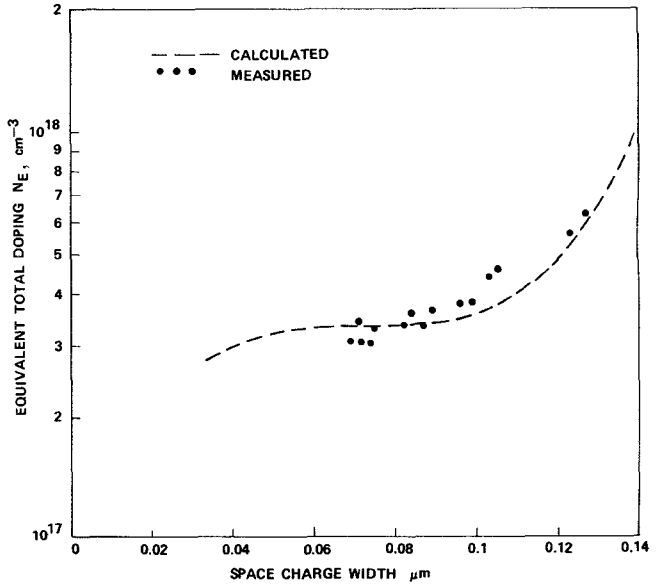

Fig. 2. Calculated and measured equivalent total doping versus space charge width of the Y-band diodes.

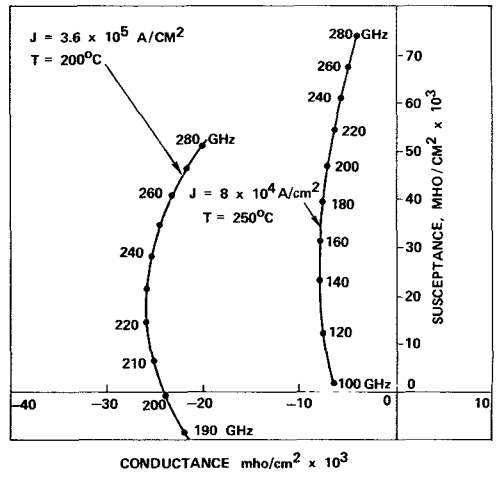

Fig. 3. Small signal admittance curves for 200-GHz double-drift IMPATT diode.

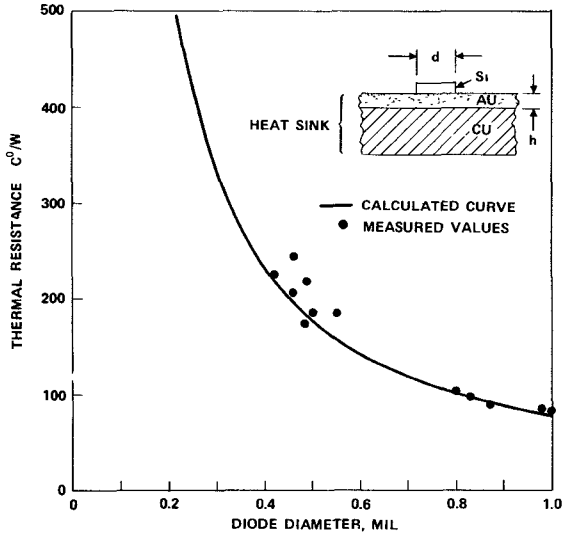

Fig. 4. Thermal resistance versus diode diameter for Y-band diodes.

Y-band diode as obtained from measurements on the epitaxial layer doping, and an estimation of the implanted p-type profile. For a DDR device the C–V method can only be used to measure an effective profile N_E given by

$$N_E^{-1} = N_D^{-1} + N_A^{-1} \tag{1}$$

where N_D and N_A are, respectively, the donor and acceptor concentrations at the edges of the depletion region formed by the application of the specified voltage. No information on N_D or N_A individually can be deduced from C–V measurements. Fig. 2 shows a plot of N_E (the "calculated" curve) based on the profile in Fig. 1 and equation (1). The plotted points in Fig. 2 are values of N_E obtained from the measured C–V data. The agreement is quite good.

Device Characterization

In order to gain understanding of the required circuit impedance level, device small-signal admittance characteristics have been calculated with a computer program [6]. Results are shown in Fig. 3. Several approximations have been used in the calculation. A symmetrical double-drift structure having a doping concentration in both the p- and n-region of 5.8×10^{17} cm^{-3} is assumed. The ionization rates of Grant [7], and the drift velocities given by Canali *et al.* [8] were used in the calculation. Two operating levels which correspond approximately to the current densities and junction temperatures appropriate to the CW and pulsed modes of operation are shown in Fig. 3. A current density of 8×10^4 A/cm^2 with a junction temperature of 250°C is taken for the CW operation, and a current density four and a half times higher at a temperature of 200°C is used for pulsed mode. The calculation illustrates that the required circuit impedance is quite different for the two cases. For example, the calculated small-signal device impedance for a diode of 1 mil diameter is approximately $-0.47 - j3.6\,\Omega$ for CW operation and $-5.9 - j3.2\,\Omega$ for pulsed case. Therefore, the required package configuration for each case is quite different. This will be further discussed in the section on package development.

To achieve reliable operation, the junction temperature of a CW IMPATT diode at the operating level must be kept as low as possible. An estimate of junction temperature can be obtained from the diode thermal resistance and input power. For a given IMPATT structure, the thermal resistance depends on the diode size and composition. Thermal resistance for the Y-band diodes has been measured. The results are plotted as a function of diode diameter in Fig. 4. Also plotted is a curve of calculated thermal resistance. The calculation is based on a simple model consisting of a silicon diode chip mounted on a two-layer (Au and Cu) semi-infinite heat sink. (Because of the very small diode diameters, it is not possible to ignore the presence of the Au bonding layer which is about 4 μm thick.) The total thermal resistance R_T is given as

$$R_T = R_{Si} + R_{HS}$$

where R_{Si} is the contribution due to the silicon between the junction and heat sink and R_{HS} is the contribution from the

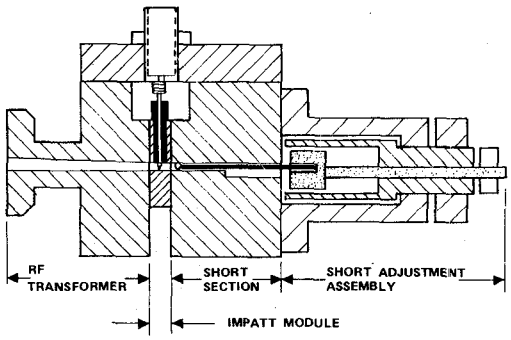

Fig. 5. Cross section of the *Y*-band IMPATT diode oscillator circuit.

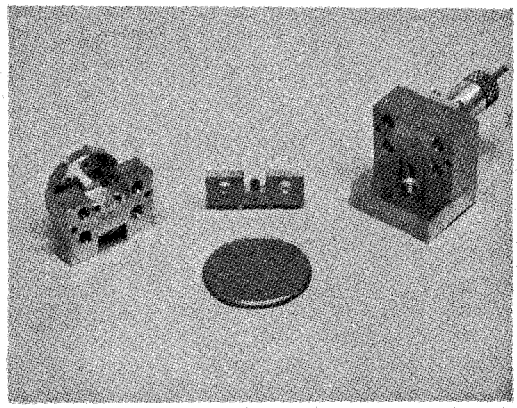

Fig. 6. Disassembled oscillator circuit left-output section with tapered waveguide transition; center wafer for mounting IMPATT diode; right tuning short section.

two-layer heat sink. The latter contribution was evaluated using an expression given by Board [9]. As can be seen, the correlation between measurement and calculation is very good.

RF Circuit Design

At *Y*-band frequencies, several problems commonly encountered at lower millimeter-wave frequencies are amplified. First, the physical dimensions of the waveguide become inconveniently small. This feature makes the diode mounting and oscillator assembly difficult. Additionally, because of the very short wavelength involved, the dimensions of the diode package become comparable to a wavelength. This fact makes impedance matching between the diode and the circuit more critically dependent on the package parameters, which can limit the performance of the diode if they are not properly chosen. In order to overcome this performance limitation, and to match the device and circuit impedance properly, the package design must be considered as an important part of the overall circuit design. The chip-level circuit design requires a new type of cavity to facilitate diode mounting and packaging.

The cross section of the *Y*-band IMPATT diode circuit designed with the above considerations is shown in Fig. 5. It consists of three major sections: a tapered waveguide section which transforms from full height to reduced height waveguide, a reduced height waveguide wafer section which contains the IMPATT diode, and a mechanical tuning short section. A photograph of the disassembled oscillator circuit is shown in Fig. 6. The cavity design resembles Sharpless wafer-type circuits used for mixer diode applications [10]. The wafer is sandwiched between the other two sections to form the complete waveguide cavity.

The use of a Sharpless wafer to mount the IMPATT diode has previously been demonstrated in a varactor-tuned oscillator [11]. For the varactor-tuned oscillator a varactor diode in a Sharpless wafer was mounted adjacent to the IMPATT wafer so that the relative coupling between the IMPATT diode and the varactor diode could be adjusted by varying the relative position of the two diodes in the plane of the cross section of the waveguide. Thus the advantage of using wafers to mount both IMPATT and varactor diodes is to achieve optimum coupling between them. For the *Y*-band IMPATT diode oscillator, the use of the wafer-mounted modular circuit permits the variation of the circuit configuration at the chip level. This is particularly important for the development of the diode package which is described in detail in the next section.

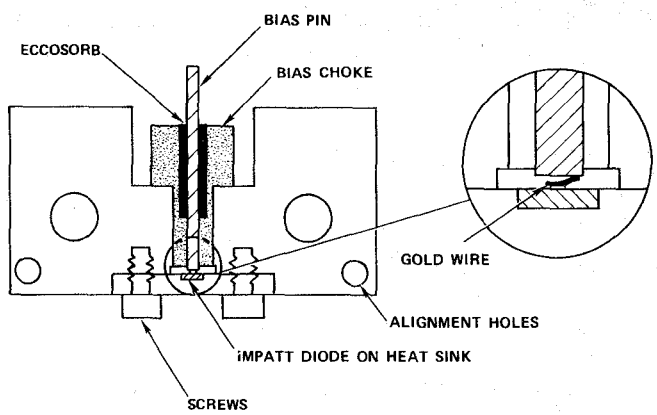

Fig. 7. Details of wafer-mounted IMPATT module.

Fig. 7 shows the details of the wafer module. The IMPATT diode is soldered to a heat-sink slab which forms the lower wall of the waveguide slot. A bias pin is used to contact the diode which can be either packaged or unpackaged. The bias pin is inserted through a choke in the top of the wafer. In order to eliminate any low-frequency instabilities, a bias network has been carefully designed as described in the following.

Bias Circuit Design

IMPATT diodes exhibit negative resistance over a wide range of frequencies which usually approaches an octave. Matching circuits with proper impedance characteristics within this frequency range work sufficiently well at small signal levels. However, at large RF levels, these circuits often produce secondary effects [12]–[18] such as excessive noise, premature saturation of output power, low efficiency, or diode burnout which seriously limit diode performance. It is apparent that the circuit impedance characteristics far outside of the negative resistance region of the diode have a significant effect on the stability of oscillators. For stable and low-noise operation, the load impedance should be well

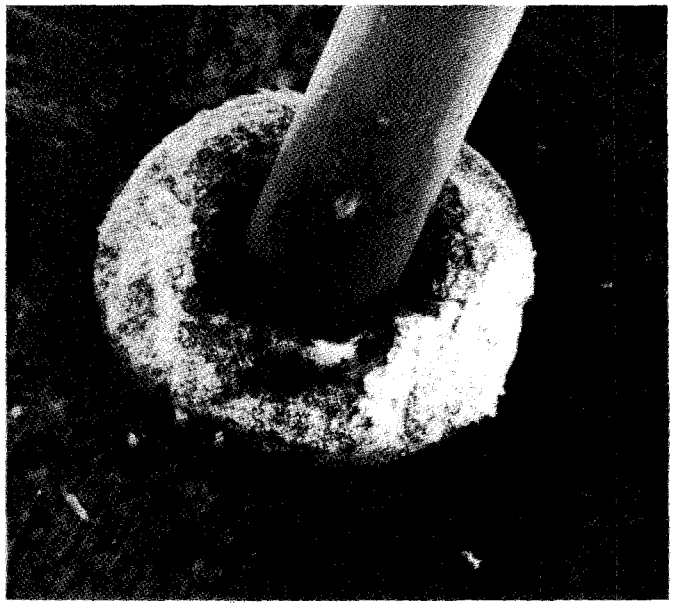

Fig. 8. SEM photograph of the bias choke with lossy material for eliminating low-frequency instabilities.

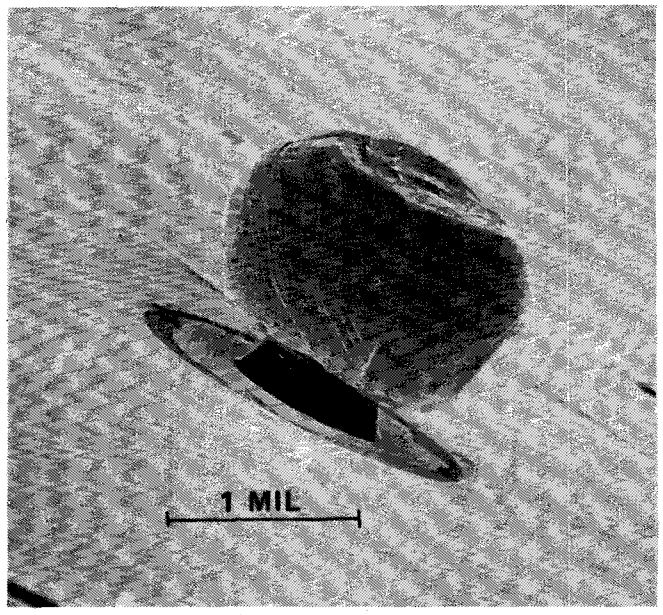

Fig. 9. Direct-contacted IMPATT diode with bonded contacting pad for *Y*-band frequencies.

controlled, from dc, up to, and above the operating frequency.

One particular source of instability often comes from the inadequate impedance characteristics of the bias network. For stable oscillation at high RF levels, a sufficiently high impedance level must be presented to the diode at all frequencies except where oscillation is desired. This often proves to be a difficult task for oscillators even at microwave and lower millimeter-wave frequencies [19]. For *Y*-band frequencies, adequate circuit-impedance characteristics must be presented to the diode over a very wide range of frequencies. This difficult task is compounded by the fact that only a stabilizing network of very small size can actually be incorporated into the thin wafer circuit. A bias choke which is made of anodized aluminum is modified by incorporating two sections of lossy material (Eccosorb[1]) as shown in Fig. 7. The two tiny tube-shaped Eccosorb sections are recessed into the back of the bias choke. Thus the circuit impedance presented to the diode at the operating frequency is not directly affected by the lossy load but the low-frequency circuit impedance is very high. This condition eliminates the bias instability. Fig. 8 is a SEM photograph of the bias choke with the lossy material. This bias network design works well even when the IMPATT oscillator is biased at a very high current level. No low-frequency instability was observed with oscillators which employ this bias network design. This is particularly important for low-noise LO applications of the oscillator.

Package Development

In order to properly transform the relatively high circuit impedance to the low device impedance, package parasitics must have optimum values. In addition, one particularly important design factor for any solid-state source in CW operation is the efficient removal of heat due to the power dissipation in the diode. The operation of IMPATT diodes at these frequencies is largely thermally limited in output power and efficiency.

In order to develop a package configuration with optimum parasitics and good thermal properties, two approaches have been used. In the first approach, bias contact is made directly to the diode without the use of a quartz standoff. Two versions of direct contact scheme have been investigated. A direct contact scheme which makes use of a resonant cap structure to contact the IMPATT diode directly has been previously demonstrated at 100 GHz [21]. Directly contacted IMPATT diodes with plated or bonded contacting pads which have been used successfully for pulsed oscillators [2] have also been investigated for CW operation with a resonant cap at *Y*-band frequencies. A SEM photograph of such a diode is shown in Fig. 9. As the frequency is increased up to and beyond 200 GHz, the realization of a precise cap shape to match the IMPATT diode at CW operation becomes difficult physically.

The required circuit admittance for a diode in CW operation is quite different from that of a pulsed device as described in the device characterization section (see Fig. 3). The required circuit susceptance for CW operation is approximately three times larger than that of the diode under high-current pulsed operation. Therefore, in contrast to the pulsed IMPATT diode which requires minimum reactive parasitics, some inductive parasitics are indeed desirable for IMPATT diodes operated in the CW mode. The appropriate inductance is apparently not easily realized with a gold ball bonded on top of the diode and contacted directly by a cap or a bias pin resonator. In addition, the scheme is not thermally adequate for CW operation. No temperature compensation mechanism exists between the bias pin and

[1] Manufactured by Emerson & Cuming, Inc.

Fig. 10. Single-welded wire contacted diode.

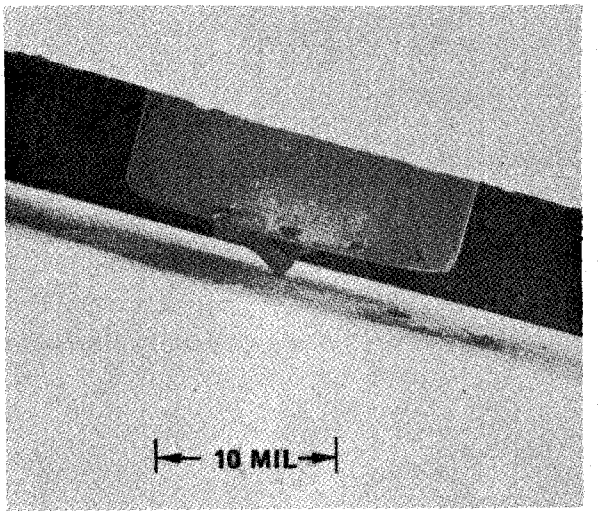

Fig. 11. Double-welded wire contacted diode.

the diode which frequently become separated from one another after the diode is turned off from an operating state of sufficiently high junction temperature. In view of these shortcomings, the resonant cap direct-contact scheme was not pursued further for CW oscillators and a second direct-contact scheme which made use of a wire welded on the end of the bias pin to contact an IMPATT chip has been investigated. Two variations of the wire configuration have been developed utilizing single- and double-welded wire contacts.

Fig. 10 shows a diode contacted by a single-welded wire on a bias pin of 7-mil diameter. The end of the bias pin is approximately 1.5 mil above the heat sink of the diode. This small pin diameter coupled with the narrow gap between the pin and the heat sink of the diode permit oscillations at very high frequencies. Oscillation as high as 250 GHz has been obtained in this configuration with diodes which normally oscillate below 200 GHz in a quartz stand-off package. A second variation of the wire configuration is shown in Fig. 11 in which an IMPATT diode mesa is directly contacted by a wire welded at two points on the end of the bias pin. This scheme results in less parasitics, but requires a larger pin diameter which limits the maximum frequency of operation to a value lower than that achievable with the single-welded wire. Both single- and double-welded wire contact schemes have shown a good current-tuning range which indicates that the parasitics associated with the wire are appropriate for CW oscillation. Moreover, the spring action of the wire provides adequate compensation for the thermal expansion and contraction which occur as the device temperature is varied between the ambient and operating values. Unfortunately, this technique requires rigid mechanical tolerances.

In a second approach, the conventional quartz standoff package previously used successfully up to 170 GHz [20] has been improved for operation at *Y*-band frequencies. Fig. 12 shows one version of such a quartz stand-off packaged IMPATT diode. It was found that the shape and size of both the ribbon and the gold "bump" are important package

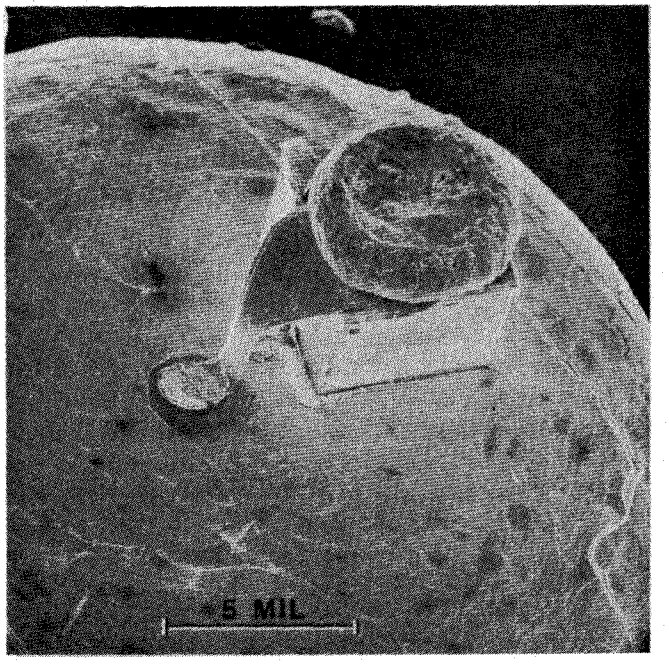

Fig. 12. Quartz standoff packaged IMPATT diode.

parameters. Diodes with this type of package give consistently good RF performance with wide tunability. This feature indicates that the parasitics of this package configuration have reasonably optimized values.

RF Measurement and Performance

Measurement of frequency is accomplished in a relatively straightforward manner using a multi-dip frequency meter consisting of a tunable resonant cavity coupled to the rectangular waveguide transmission path. A block diagram of the test setup used to measure the frequency characteristics of the source and to tune the source for the best output power at each current level is shown in Fig. 13. The output waveguide of the CW source has a WR-4 dimension (*Y*-band) with a UG387 modified flange. A *Y*-band flange

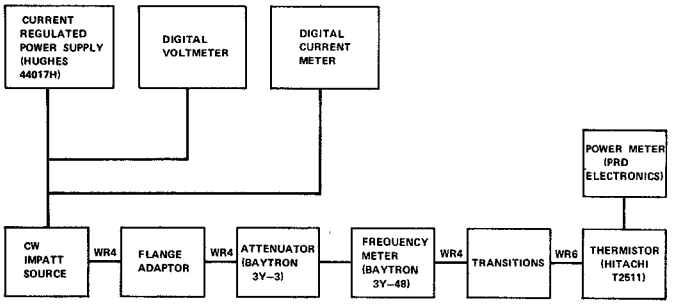

Fig. 13. Setup for measuring frequency and tuning for optimum power.

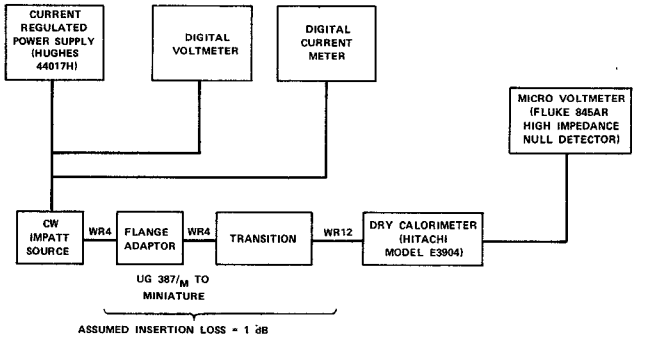

Fig. 14. Test setup for measuring RF output power.

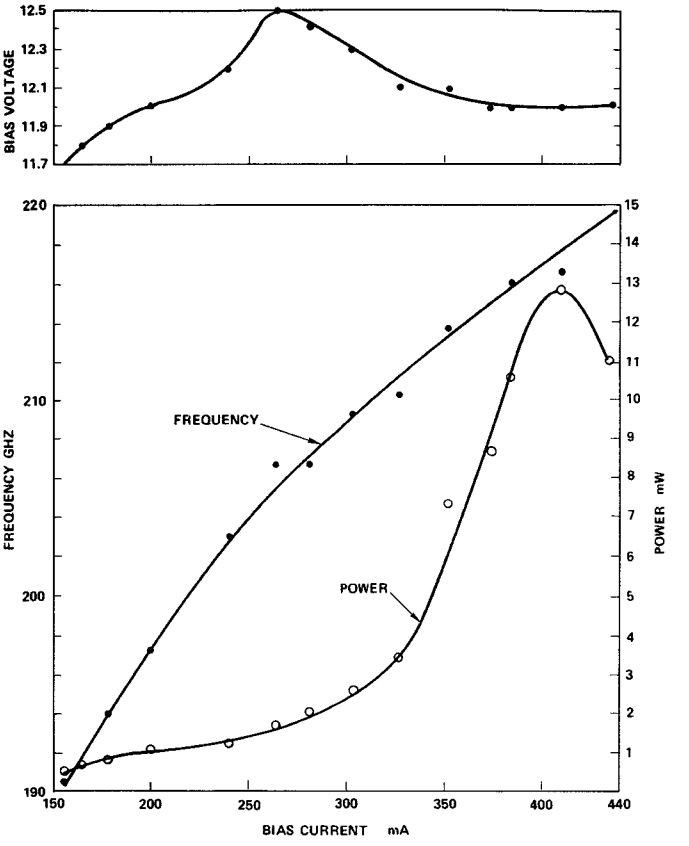

Fig. 15. Tuning characteristics of a Y-band IMPATT oscillator.

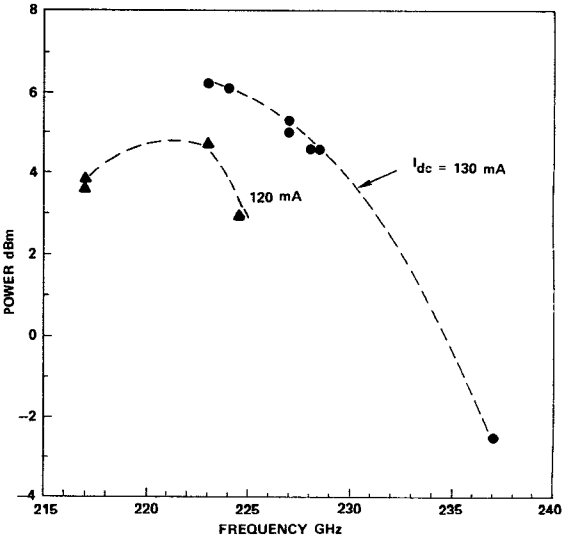

Fig. 16. Mechanical tuning characteristics of a Y-band IMPATT oscillator.

adaptor is used between the UG387 modified flange and a miniature flange which is compatible with most commercially available test equipment.

The test setup for measuring RF output power is shown in Fig. 14. An E-band (WR-12) dry calorimeter has been used to estimate the output power. It has been calibrated at dc, and at 60 GHz. It has an output-to-input conversion factor of 65.5 μV/mW at dc and 61.78 μV/mW at 60 GHz. The latter factor has been assumed to be valid for Y-band operation. Another assumption involved in the RF power measurement is the insertion loss associated with the waveguide sections which connect the source to the dry calorimeter. Since the output of the source is in WR4 waveguide with a UG 387 modified flange, a flange adaptor and a waveguide transition have been used to connect the source to the dry calorimeter. The insertion loss of these two sections of waveguide has been conservatively estimated to be 1 dB.

Oscillators with the circuit and package designs described above have been evaluated extensively in Y-band with the silicon double-drift IMPATT diode at a junction temperature of approximately 250°C above the ambient. CW powers of 23 mW at 207 GHz, 10 mW at 230 GHz, and 1.9 mW at 250 GHz have been achieved.

Particular emphasis is placed on the tunability of the oscillator for system applications. Fig. 15 shows the RF performance of a mechanically tuned oscillator with a quartz standoff packaged IMPATT diode as a function of bias current. The frequency of oscillation increases monotonically from approximately 190 to 220 GHz as the bias current is varied from 150 to 440 mA. It is interesting to point out that there are no low-frequency instabilities observed, even though there is low-frequency negative resistance induced by the combination of RF rectification effects and space charge effects at the high current levels. The stability can be attributed to the special bias network used. Fig. 16 shows the mechanical tuning characteristics of an IMPATT diode chip of 11-μm diameter contacted directly by a double-welded wire on a 11.8-mil diameter bias pin. A total

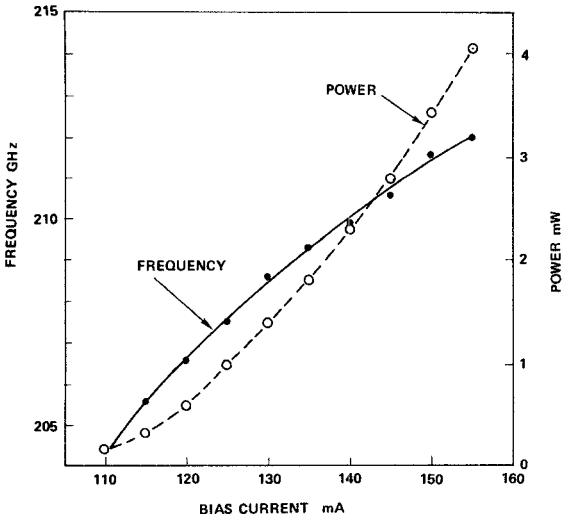

Fig. 17. Bias-tuned IMPATT oscillator above 200 GHz.

mechanical tuning range of 14 GHz has been achieved at a fixed bias current of 130 mA. Bias-current-tuned oscillators have also been studied. Fig. 17 shows the bias tuning characteristics of a double-drift IMPATT diode in a quartz standoff package. An electronic tuning range of 7 GHz with a maximum power of 4 mW has been achieved.

No attempt has been made to measure the noise characteristics of the *Y*-band IMPATT oscillators. However, a 208-GHz 7-mW IMPATT oscillator constructed with device and circuit techniques described here, has been used as LO for testing a quasi-optical radiometric receiver. The noise performance of the IMPATT oscillator exceeds that of the best available klystron when a quasi-optical transmission filter is used in conjunction with the IMPATT source [22].

Conclusion

The development of solid-state oscillators in *Y*-band frequencies has been described. Ion-implanted double-drift IMPATT diodes with p^+-p-n-n^+ doping profile have been developed for operation in *Y*-band frequencies. Special attention has been given to substrate thinning, and to minimizing unswept active regions. Calculations of device small-signal impedance have been performed to gain some understanding of the required circuit impedance level, and to aid package development. Characterization of device thermal impedance to ensure reliable operation has also been performed. A wafer-mounted IMPATT module which permits the variation of the circuit configuration at the chip level has been adapted for this work. A new bias choke design has also been developed and incorporated into the thin wafer. No low-frequency instability was observed with oscillators which employ this bias network design. A variety of package configurations have been investigated. Both direct contact schemes and conventional quartz standoff packages have been developed for *Y*-band frequencies. A tuning range of nearly 30 GHz has been achieved with an IMPATT diode in an improved quartz standoff package. This feature implies that the parasitics of this package configuration have reasonably optimized values.

Acknowledgment

The authors wish to thank Dr. T. A. Midford for his encouragement and helpful suggestions. They also wish to thank H. Luckey, A. Martin, and M. Morishita for their excellent technical assistance.

References

[1] T. Ishibashi and M. Ohmori, "200 GHz 50 mW CW oscillator with silicon IMPATT diodes," *IEEE Trans. Microwave Theory Tech.*, vol. MTT-24, pp. 858–859, Nov. 1976.

[2] C. Chao, R. L. Bernick, R. S. Ying, K. P. Weller, D. H. Lee, and E. M. Nakaji, "Pulsed IMPATT diode oscillators above 200 GHz," in *IEEE Int. Solid-State Circuits Conf. Dig.* (Philadelphia, PA), pp. 130, 131, Feb. 1977.

[3] C. Chao, R. L. Bernick, E. M. Nakaji, R. S. Ying, K. P. Weller, and D. H. Lee, "*Y*-band (170–260 GHz) tunable CW IMPATT diode oscillators," in *IEEE Int. Microwave Symp. Dig.* (San Diego, CA), pp. 26–28, June 1977.

[4] D. H. Lee *et al.*, "Ion-implanted profiles for high-frequency (>100 GHz) IMPATT diodes," in *Proc. 4th Int. Conf. Ion Implanation in Semiconductors and Other Materials* (Osaka, Japan), pp. 167–168.

[5] B. C. Deloach, Jr., "Thin skin IMPATTs," *IEEE Trans. Microwave Theory Tech.*, vol. MTT-18, pp. 72–74, Jan. 1970.

[6] T. Misawa, "Negative resistance in p-n junction under avalanche breakdown conditions, Parts I and II," *IEEE Trans. Electron Devices*, vol. ED-13, pp. 137–151, Jan. 1966.

[7] W. N. Grant, "Electron and hole ionization rates in epitaxial silicon at high electric fields," *Solid-State Electron.*, vol. 16, pp. 1189–1203, 1973.

[8] C. Canali, G. Majni, R. Minder, and G. Ottaviani, "Electron and hole drift velocity measurements in silicon and their empirical relation to electric field and temperature," *IEEE Trans. Electron Devices*, vol. ED-22, pp. 1045, 1046, Nov. 1975.

[9] K. Board, "Thermal properties of annular and array geometry semiconductor devices on composite heat sinks," *Solid-State Electron.*, vol. 16, pp. 1315–1320, 1973.

[10] W. M. Sharpless, "Wafer-type millimeter-wave rectifiers," *Bell Syst. Tech. J.*, vol. 35, no. 6, pp. 1385–1420, Nov. 1956.

[11] T. P. Lee and R. D. Standley, "Frequency modulation of millimeter-wave IMPATT diode oscillator and related harmonic generation effects," *Bell Syst. Tech. J.*, vol. 48, no. 1, pp. 143–161, Jan. 1969.

[12] M. E. Hines, "Large-signal noise, frequency conversion, and parametric instabilities in IMPATT diode networks," *Proc. IEEE*, vol. 60, no. 12, pp. 1534–1548, Dec. 1972.

[13] C. A. Brackett, "The elimination of tuning-induced burnout and bias-circuit oscillations in IMPATT oscillators," *Bell Syst. Tech. J.*, vol. 52, no. 3, pp. 271–306, Mar. 1973.

[14] W. E. Schroeder, "Spurious parametric oscillations in IMPATT diode circuits," *Bell Syst. Tech. J.*, vol. 53, no. 7, pp. 1187–1210, Sept. 1974.

[15] J. Gonda and W. E. Schroeder, "IMPATT diode circuit design for parametric stability," *IEEE Trans. Microwave Theory Tech.*, vol. MTT-25, pp. 343–352, May 1977.

[16] J. J. Goedbloed and H. Tjassens, "Parasitic oscillations in IMPATT-diode oscillators," in *Proc. 4th European Microwave Conf.* (Montreux, Switzerland), pp. 328–332, Sept. 1974.

[17] J. J. Goebloed, "Investigation of parasitic oscillations in IMPATT-diode oscillators by a simple locus chart," *Electron. Lett.*, vol. 11, no. 3, Feb. 6, 1975.

[18] G. S. Hobson and R. C. Tozer, "Spurious oscillations in IMPATT oscillators," *Electron. Lett.*, vol. 11, no. 14, p. 291, July 10, 1975.

[19] Y. Hirachi, T. Nakagami, Y. Toyama, and Y. Fukukawa, "High-power 50 GHz double-drift-region IMPATT oscillators with improved bias circuits for eliminating low-frequency instabilities," *IEEE Trans. Microwave Theory Tech.*, vol. MTT-24, pp. 731–737, Nov. 1976.

[20] K. P. Weller, R. S. Ying, and D. H. Lee, "Millimeter IMPATT sources for the 130–170 GHz range," *IEEE Trans. Microwave Theory Tech.*, vol. MTT-24, pp. 738–743, Nov. 1976.

[21] T. Misawa and L. P. Marinaccio, "100 GHz Si IMPATT diodes for CW operation," in *Proc. Symp. on Submillimeter Waves*, pp. 53–67, 1970.

[22] J. Gustincic, private communication.